

000 001 002 003 004 005 006 007 008 009 010 011 012 013 014 015 016 017 018 019 020 021 022 023 024 025 026 027 028 029 030 031 032 033 034 035 036 037 038 039 040 041 042 043 044 045 046 047 048 049 050 051 052 053 GAIA: A DATA FLYWHEEL SYSTEM FOR TRAINING GUI TEST-TIME SCALING CRITIC MODELS

005 **Anonymous authors**

006 Paper under double-blind review

ABSTRACT

011 While Large Vision-Language Models (LVLMs) have significantly advanced GUI
012 agents' capabilities in parsing textual instructions, interpreting screen content, and
013 executing tasks, a critical challenge persists: the irreversibility of agent operations—
014 where a single erroneous action can trigger catastrophic deviations. To
015 address this, we propose the GUI Action Critic's Data Flywheel System (GAIA),
016 a training framework that enables the models to have iterative critic capabilities,
017 which are used to improve the Test-Time Scaling (TTS) of basic GUI agents' per-
018 formance. Specifically, we train an **Intuitive Critic Model** (ICM) using positive
019 and negative action examples from a base agent first. This critic evaluates the im-
020 mediate correctness of the agent's intended actions, thereby selecting operations
021 with higher success probability. Then, the initial critic guides agent actions to
022 collect refined positive/negative samples, initiating the self-improving cycle. The
023 augmented data then trains a second-round critic with enhanced discernment ca-
024 pability. We conduct experiments on various datasets and demonstrate that the
025 proposed ICM can improve the test-time performance of various closed-source
026 and open-source models, and the performance can be gradually improved as the
027 data is recycled. The code and dataset will be publicly released.

1 INTRODUCTION

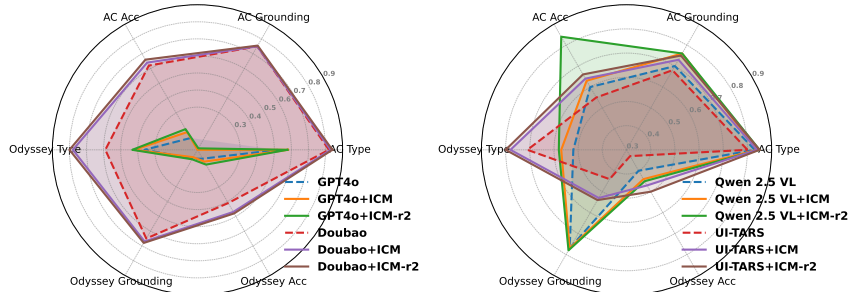
031 The automation of Graphical User Interface (GUI) interactions represents a critical frontier in de-
032 veloping intelligent digital assistants (Wang et al., 2024b; Hu et al., 2024; Nguyen et al., 2024).
033 Recent breakthroughs in Large Vision-Language Models (LVLMs) (Wang et al., 2024a; Bai et al.,
034 2025), leveraging advanced post-training techniques, have substantially enhanced agents' capabili-
035 ties in interpreting natural language commands, perceiving visual elements, and executing multi-step
036 tasks (Hong et al., 2024; Cheng et al., 2024). Within this rapidly evolving landscape, the develop-
037 ment of robust GUI agents has largely converged on two primary methodological paradigms. The
038 first approaches (Wu et al., 2025c; Xu et al., 2024; Qin et al., 2025; Liu et al., 2025a) train models
039 through Supervised Fine-Tuning (SFT) to directly align their behavior with predefined task ob-
040 jectives. The second approaches employ Reinforcement Fine-Tuning (RFT) (Lu et al., 2025; Xia
041 & Luo, 2025; Liu et al., 2025b), which significantly enhances generalization in complex tasks by
adopting a reasoning format.

042 Despite these advances, the dynamic and continuous nature of real-world GUI tasks means that
043 agents can still produce ambiguous or incorrect action proposals at any step. **A single mis-click**
044 **or mis-typed output can be irreversible**, derailing the entire workflow and leaving the system
045 in an unrecoverable state. This high-stakes environment imperatively demands **a mechanism for**
046 **pre-execution validation**.

047 To avoid irreversible errors in execution and improve the performance of basic GUI agents during
048 testing, previous studies have designed action verifiers for GUI agents (Wu et al., 2025b; Xiao et al.,
049 2025; Yang et al., 2025), **which are used to determine the correctness of multiple actions rolled out by**
050 **GUI agents, and then filter out incorrect candidates**. However, these existing implementations suffer
051 from two primary limitations. First, training a correctness verifier requires defining positive and
052 negative action samples. Existing work on defining negative samples relies on heuristic algorithms,
053 such as randomly selecting click locations on the current screenshot (Xiao et al., 2025), which fails to
capture the realistic action distribution and leads to suboptimal judgment performance. Second, the



(a) The promotion process of the critic model to the GUI Agent during testing.



(b) Comparison of high-level task performance improvements on closed-source and open-source GUI Agents.

Figure 1: **Intuitive results.** ICM guides agents' action during testing, as shown in (a), thereby improving the agent's accuracy, and is continuously improved by the data flywheel, as shown in (b).

reasoning-based verifiers (Wanyan et al., 2025) implemented in existing work violate the intuitive properties of binary judgments. For an intuitive correctness judgment problem, biological research suggests that higher-level judgment pathways are often more adept than performing extensive multi-step reasoning (Liu & Pleskac, 2011; Poldrack et al., 2005; Doyon & Benali, 2005), which indicates that excessive reasoning can be less effective (Bilalić et al., 2008; Wan et al., 2011). Furthermore, reasoning-based judgment outputs more tokens, thereby reducing the efficiency of test-time scaling.

To fully leverage pre-execution evaluation to enhance GUI agent capabilities and execution correctness, we developed a **GUI Action Critic’s Data Flywheel System (GAIA)**. This system comprises two core phases: the initialization phase (Phase 1) and the iteration phase (Phase 2), yielding the **Intuitive Critic Model (ICM)**. In **Phase 1**, we use real GUI agents to act on an existing dataset to collect positive and negative action data that are random but consistent with the behavior distribution. Using this binary-labeled action dataset, we train ICM to assess action correctness given environmental context. In **Phase 2**, as illustrated in Figure 1(a), ICM employs a Best-of-N approach to select the highest-probability correct actions from agent rollouts. While ICM guidance significantly improves action accuracy, challenging samples persist and produce errors. These difficult cases are annotated and fed back into the data flywheel. Through iterative data augmentation, the flywheel continuously incorporates new action samples, progressively covering challenging scenarios within the action space. Driven by this enriched dataset, we train an enhanced critic—Intuitive Critic Model on Round Two (ICM-r2)—which achieves higher discriminative accuracy for more precise behavioral guidance. This establishes a self-evolutionary virtuous cycle between the data flywheel and critic models, continuously improving GUI agent action accuracy.

Leveraging the proposed system GAIA, ICM achieves SOTA performance in action critique. Naturally, we integrate it into Test-Time Scaling (TTS) (Snell et al., 2025; Chen et al., 2024b; Snell et al., 2024; Prabhudesai et al., 2023; Wang et al., 2025; Tian et al., 2025) during inference, where ICM evaluates stochastically generated actions from the TTS process, **releasing only executes the action if it is judged to be correct and has the highest probability of the correct token**. Furthermore, based on GAIA’s comprehensive definition, ICM can evaluate the correctness of actions across the entire space, rather than being limited to the accuracy of click actions in grounding tasks Yang et al. (2025); Wu et al. (2025a). To validate the framework’s general applicability, we conduct joint experiments using mainstream GUI Agents (including GPT-4o (Hurst et al., 2024) and UI-TARS (Qin et al., 2025)) on several GUI Agent benchmarks.

As shown by the comparative results in Figure 1 (b), the guidance from our iteratively evolved critic models (ICM and ICM-r2) leads to significant performance improvements in basic GUI agents, including GUI operation task planning and grounding capabilities.

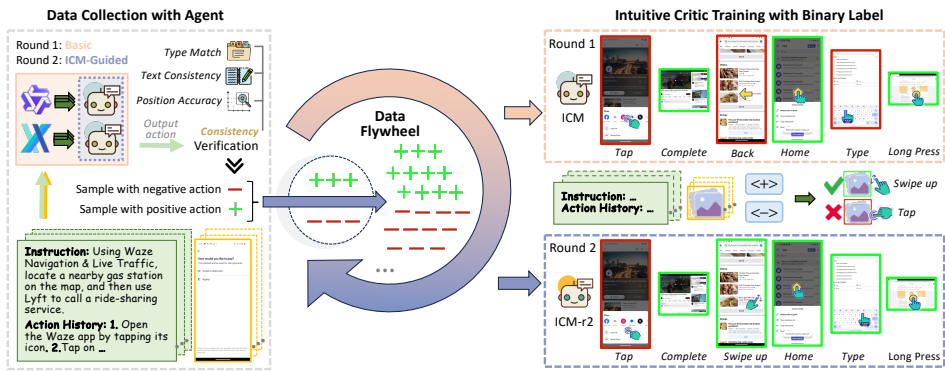


Figure 2: **Data flywheel curation pipeline for GAIA.** A sample dataset is constructed using GUI agent interactions. The positive and negative labels are marked by comparing the ground truth actions to train an action correctness discrimination model. After the critic model guides the GUI agent, it further expands the dataset, pushing the data flywheel to cover more action distributions, thereby promoting the iterative improvement of model performance.

Overall, the main contributions are summarized as follows:

1. We introduce GAIA—a novel Data Flywheel System designed for training GUI action-critic models. By iteratively curating positive and negative samples from real-world action data, GAIA continuously boosts model performance and robustness.
2. We propose the ICM for GUI interaction tasks, a critic model trained on data curated by our data flywheel. The ICM enhances the performance of existing GUI agents by employing a best-of-N approach to select the most probable correct action with TTS. This initial boost is then continuously refined as the ICM’s discriminatory accuracy is iteratively improved by the data flywheel.
3. We comprehensively demonstrate across multiple datasets that ICM trained with our proposed GAIA system significantly enhances the overall performance of both closed-source and open-source GUI agents.

2 RELATED WORK

2.1 GUI AGENT

The development of autonomous agents powered by LLMs and LVLMs has significantly advanced interactive functionalities within digital environments. Early GUI systems primarily leveraged LLMs to interpret structured representations (Hong et al., 2024; Nong et al., 2024; Song et al., 2024). The development of LVLM simplifies the paradigm, allowing GUI agents to receive raw visual signals from the screenshots (Hu et al., 2024; Liu et al., 2024; Shen et al., 2024; Tang et al., 2025; Christianos et al., 2024; Zheng et al., 2025; Gou et al., 2024; Wu et al., 2025c). Recent efforts, such as Aguvis (Xu et al., 2024) and UI-TARS (Qin et al., 2025), have advanced autonomous GUI navigation by integrating explicit planning, sophisticated reasoning, and GUI-specific pretraining to handle complex digital environments. Concurrently, the advent of rule-based Reinforcement Learning (RL) approaches (Jaech et al., 2024; Guo et al., 2025) has further enhanced GUI agent capabilities. These RFT methods improve reasoning and generalization by enabling models to learn universal action strategies from high-quality samples (Liu et al., 2025c; Shen et al., 2025; Lu et al., 2025; Xia & Luo, 2025; Liu et al., 2025b). While fine-tuning and model scaling can enhance GUI agent capabilities, these methods are often prohibitively resource-intensive. This highlights a clear need for test-time enhancements that can offer universal performance improvements across various agent models without costly retraining.

162
163

2.2 CRITIC MODEL

164 To solve the problem of suboptimal single-shot model output (Zhang et al., 2025b; Martino et al.,
 165 2023; Wen et al., 2024; Chen et al., 2024a), research has gradually focused on improving the per-
 166 formance of the basic model during testing with the help of the critic model (McAleese et al., 2024; Ji
 167 et al., 2023; Kalyanpur et al., 2024; Zhang et al., 2025a; Xiong et al., 2025). This concept has been
 168 expanded to the GUI domain with notable works like GUI-Genie (Xiao et al., 2025), GUI-Actor (Wu
 169 et al., 2025b), GTA1 (Yang et al., 2025), and GUI-Critic-R1 (Wanyan et al., 2025). However, ex-
 170 isting GUI critics often rely on synthetic data generated by heuristic algorithms, such as randomly
 171 selecting click locations (Wu et al., 2025b), cross-task substitution, or early truncation (Xiao et al.,
 172 2025). This approach fails to accurately simulate the complex behavior of real GUI agents across
 173 the full action space, thereby preventing the critic from learning faithful discrimination criteria. Fur-
 174 thermore, while some approaches use RL to inject reasoning capabilities into the critic (Wanyan
 175 et al., 2025), this often contradicts the very motivation for intuitive judgment (Liu & Pleskac, 2011;
 Wan et al., 2011) and introduces delays due to extended output token generation.

176
177

3 METHOD

178

179 In this section, we detail the design of our data flywheel-driven GAIA system for the GUI agent
 180 shown in Figure 2. We begin in Section 3.1 by introducing the general definition of the GUI agent
 181 task and the crucial role of the critic model. Section 3.2 delves into the design and application of our
 182 data flywheel system within the initial round of the evaluation process. In Section 3.3, we present
 183 the model training in the second round, which builds upon the outcomes from the first iteration and
 184 forms a virtuous cycle.

185

3.1 PRELIMINARIES

186

187 The interaction between a GUI agent and its environment can be formulated as a Markov Decision
 188 Process (MDP), denoted by the tuple $\langle \mathcal{S}, \mathcal{A}, \mathcal{Z}, \mathcal{T}, \mathcal{O} \rangle$. Here, \mathcal{S} defines the state space of possible
 189 screen states, while \mathcal{A} encompasses the action space, including interaction types like clicking, typ-
 190 ing, and scrolling. The observation space \mathcal{Z} captures inputs such as screenshots or structured UI
 191 representations. The state transition probability is given by $\mathcal{T} : \mathcal{S} \times \mathcal{A} \times \mathcal{S} \rightarrow [0, 1]$, mapping a
 192 state and action to a new state. Similarly, $\mathcal{O} : \mathcal{S} \times \mathcal{A} \rightarrow \mathcal{Z}$ describes the likelihood of observing a
 193 particular output given a state and an action. During GUI task execution, at each discrete time step
 194 t , the agent receives an input tuple (z_t, u, h) , comprising the current screen observation $z_t \in \mathcal{Z}$, the
 195 global task instruction u , and the accumulated interaction history h . The agent’s decision-making
 196 process for GUI actions is then formalized by a structured policy function \mathcal{F} :

197

$$\mathcal{F}(z_t, u, h) \rightarrow o_t = \{a_t, c_t\}, \quad (1)$$

198

199 where o_t represents the agent output at time t , consisting of the action type a_t (e.g., click, scroll,
 200 and type) and its corresponding parameters c_t (e.g., click coordinates, text content for typing). After
 201 a_t is executed, the environment transitions to a new state z_{t+1} , and this iterative process continues
 202 until the task is successfully completed or a predefined termination condition is met.

202

203 The proposed ICM, building upon the same observations and the GUI agent’s current proposed
 204 action o_t , outputs a judgment j_t regarding the correctness of that action:

205

$$\mathcal{J}(o_t | (z_t, u, h)) \rightarrow \{j_t, p_t\}, \quad (2)$$

206

207 where j_t is a binary indicator, “*correct*” for correct actions and “*wrong*” for incorrect, p_t represents
 208 the probability of the judgment, which supports finding the correct action with the highest confi-
 209 dence. By enabling the sampling of multiple candidate actions and prioritizing them based on their
 210 respective correctness probabilities, ICM ensures that a more optimal action for the current state is
 211 selected and executed, significantly enhancing the agent’s actual success rate.

212

3.2 ACTION DECISION WITH INTUITIVE CRITIC

213

3.2.1 DATA CURATION

214

215 To enable the judgment model to distinguish the correctness of real actions, we meticulously define
 216 both positive and negative samples of GUI agent actions. We begin by having existing GUI agents

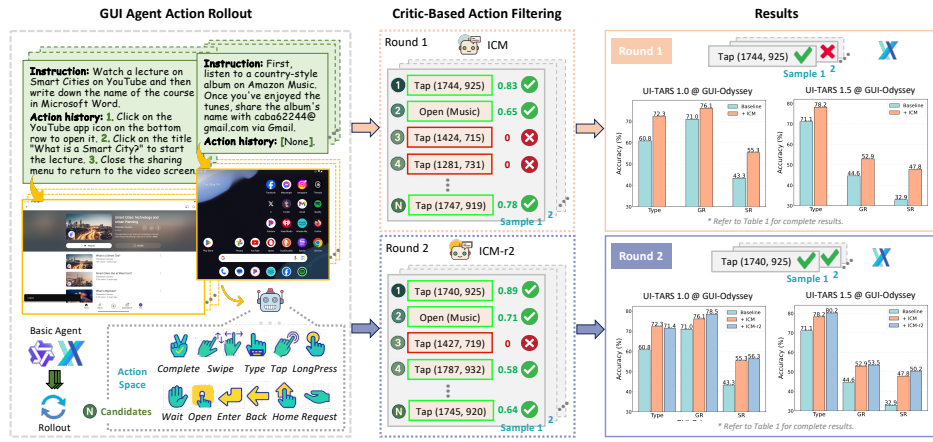


Figure 3: **Test-Time scaling pipeline.** Through best-of- N rollout, multi-candidate actions of GUI agents are given, and the correct action with the highest probability is selected after ICM evaluation.

$\Pi = \{\pi_1, \pi_2, \dots, \pi_i\}$ (Qin et al., 2025) interact with and traverse publicly accessible datasets (Li et al., 2024; Lu et al., 2024), allowing us to collect authentic, step-level operations across various GUI scenarios. The datasets used are static and well-defined, meaning that each single-step action has a ground truth label to indicate the action the agent should take in the corresponding environment. Minor deviations in action parameters, such as slight offsets in click coordinates and semantic deviations in input text, are also guaranteed by recognized validation rules Wu et al. (2025c). For each action executed in a specific state (z, u, h) , we then leverage ground truth labels to determine its correctness. An action is designated positive (with a correctness judge $j = \text{"correct"}$) if it aligns with the GT.

Conversely, we identify negative samples (with a correctness score $j = \text{"wrong"}$) based on states where the agent’s action deviates from the GT. This approach ensures that our collected negative operations are closely aligned with the actual error distribution observed in real GUI environments, significantly enhancing the quality and realism of our training dataset. To prevent bias during ICM training, we balance the collected positive and negative samples, ensuring an equal 50% split for each. This carefully curated dataset, denoted as $\mathcal{D} = \{j_k | z_k, u_k, h_k, o_k^{\pi_i}\}_{k=1}^K$, forms the foundation of our data flywheel GAIA.

3.2.2 ICM TRAINING AND GUIDANCE

Based on the dataset \mathcal{D} , ICM is trained to intuitively judge the correctness of actions. Specifically, the input of ICM includes the screen observation z_k , the instruction description u_k , the action history h_k , and the given agent action $o_k^{\pi_i}$. We implement ICM using LVLM and use standard cross-entropy loss to supervise the ICM’s output tokens. For each sample in our dataset \mathcal{D} , the model’s output is a token representing either "correct" or "wrong" . The training process aims to minimize the discrepancy between the model’s predicted probability and the ground truth label:

$$\mathcal{L}_{\text{CE}} = -\frac{1}{K} \sum_{k=1}^K \left[j_k \log (P_{\theta_c}(\text{"correct"} | z_k, u_k, h_k, o_k^{\pi_i})) \right. \\ \left. + (1 - j_k) \log (1 - P_{\theta_c}(\text{"correct"} | z_k, u_k, h_k, o_k^{\pi_i})) \right], \quad (3)$$

where $P_{\theta_c}(\text{"correct"} | z_k, u_k, h_k, o_k^{\pi_i})$ represents the probability assigned by the critic model θ_c to the "correct" token.

During test-time, a GUI agent π_i generates N candidate actions $\mathcal{O} = \{o_1, \dots, o_N\}$ through N -rollout sampling. ICM evaluates these candidates by assigning each action a correctness judge j_n and a potential confidence score represented by the token probability p_n . Leveraging the best-of- N filtering strategy, we select the optimal action o^* from the subset of correct candidates $\mathcal{O}_{\text{correct}}$ that

270 **Table 1: GUI planning accuracy on AndroidControl and GUI-Odyssey.** \dagger represents the closed-
 271 source UI-TARS 1.5 called through the Doubao API. $*$ represents an agent that reproduces the open-
 272 source model. \uparrow and \downarrow respectively represent the performance changes relative to the base agents.
 273

274 Model	275 Method	276 Size	277 AndroidControl-Low			278 AndroidControl-High			279 GUI-Odyssey		
			280 Type	281 GR	282 SR	283 Type	284 GR	285 SR	286 Type	287 GR	288 SR
OS-Atlas-Base	ZS	7B	73.0	73.4	50.9	57.4	54.9	29.8	60.4	39.7	27.0
SeeClick	SFT	9.6B	93.0	73.4	75.0	82.9	62.9	59.1	71.0	52.4	53.9
Aria-UI	SFT	3.9B	—	87.7	67.3	—	43.2	10.2	—	86.8	36.5
Aguvis	SFT	7B	—	—	80.5	—	—	61.5	—	—	—
UI-R1	RFT	3B	79.2	82.4	66.4	57.9	55.7	45.4	52.2	34.5	32.5
GUI-R1	RFT	3B	83.7	81.6	64.4	58.0	56.2	46.6	54.8	41.5	41.3
GPT4o			—	78.8	8.0	20.4	52.4	3.6	13.2	36.6	11.4
	+ ICM		82.4 \uparrow 3.6	9.2 \uparrow 1.2	24.8 \uparrow 4.4	58.0 \uparrow 5.6	5.3 \uparrow 1.7	17.0 \uparrow 3.8	42.9 \uparrow 6.3	10.0 \downarrow 1.6	13.4 \uparrow 2.0
	+ ICM-r2		81.6 \uparrow 2.8	8.5 \uparrow 0.5	23.8 \uparrow 3.4	57.6 \uparrow 5.2	6.1 \uparrow 2.5	18.8 \uparrow 5.6	43.2 \uparrow 6.6	11.4 \downarrow 0.2	14.5 \uparrow 3.1
Doubao \dagger			—	97.0	86.4	86.2	82.0	75.0	62.4	67.1	67.3
	+ ICM		97.0	—	86.6 \uparrow 0.2	86.4 \uparrow 0.2	83.2 \uparrow 1.2	75.1 \uparrow 0.1	64.4 \uparrow 2.0	70.1 \uparrow 3.0	68.4 \uparrow 1.1
	+ ICM-r2		96.6 \downarrow 0.4	86.6 \uparrow 0.2	86.0 \downarrow 0.2	84.2 \uparrow 2.2	75.5 \uparrow 0.5	66.0 \uparrow 3.6	71.6 \uparrow 4.5	68.0 \uparrow 0.7	47.9 \uparrow 4.1
Qwen 2.5 VL		7B	94.4	85.6	81.8	83.0	70.9	60.6	52.7	77.2	40.2
	+ ICM		95.4 \uparrow 1.0	86.0 \uparrow 0.4	81.2 \downarrow 0.6	84.0 \uparrow 1.0	75.9 \uparrow 5.0	63.4 \uparrow 2.8	57.3 \uparrow 4.6	77.2 —	43.7 \uparrow 3.5
	+ ICM-r2		94.6 \uparrow 0.2	85.4 \downarrow 0.2	81.8 —	84.4 \uparrow 1.4	75.9 \uparrow 5.0	63.8 \uparrow 3.2	58.1 \uparrow 5.4	78.3 \uparrow 1.1	44.8 \uparrow 4.6
UI-TARS 1.0*		7B	90.0	85.1	75.4	80.8	68.9	58.2	60.8	71.0	43.3
	+ ICM		90.5 \uparrow 0.5	87.6 \uparrow 2.5	80.4 \uparrow 5.0	82.3 \uparrow 1.5	79.5 \uparrow 10.6	67.5 \uparrow 9.3	72.3 \uparrow 11.5	76.1 \uparrow 5.1	55.3 \uparrow 12.0
	+ ICM-r2		90.0	—	86.8 \uparrow 1.7	80.2 \uparrow 4.8	82.7 \uparrow 1.9	78.9 \uparrow 10.0	67.1 \uparrow 8.9	71.4 \uparrow 10.6	78.5 \uparrow 7.5
UI-TARS 1.5*		7B	86.4	82.4	72.2	80.2	68.1	55.8	71.1	44.6	32.9
	+ ICM		90.3 \uparrow 3.9	85.0 \uparrow 2.6	79.0 \uparrow 6.8	84.2 \uparrow 4.0	73.3 \uparrow 5.2	64.5 \uparrow 8.7	78.2 \uparrow 7.1	52.9 \uparrow 8.3	47.8 \uparrow 14.9
	+ ICM-r2		90.1 \uparrow 3.7	85.5 \uparrow 3.1	79.2 \uparrow 7.0	84.6 \uparrow 4.5	74.7 \uparrow 3.8	65.6 \uparrow 7.4	80.2 \uparrow 9.1	53.5 \uparrow 8.9	50.2 \uparrow 17.3

294 is judged as correct and whose corresponding “*correct*” token has the highest probability p_n :
 295

$$296 o^* = \begin{cases} \arg \max_{o_n \in \mathcal{O}_{\text{correct}}} p_n, & \text{if } \mathcal{O}_{\text{correct}} \neq \emptyset \\ 297 o_1. & \text{otherwise} \end{cases} \quad (4)$$

298 This approach effectively guides the agent to bypass single-shot output failures and select the most
 299 promising action, thereby significantly boosting its overall execution accuracy.
 300

301 3.3 DATA FLYWHEEL AND CRITIC SCALING

302 Guided by Equation 4, the execution accuracy has been significantly improved. However, some
 303 difficult action samples require more precise judgment. Considering that ICM and test-time scal-
 304 ing performance can be further enhanced with data, we collect agent actions guided by ICM
 305 and, after filtering for positive and negative balance, add them to the data flywheel to form
 306 $\mathcal{D}^+ = \{j_k | z_k, u_k, h_k, o_k^{\pi_k}, \theta_c\}_{k=1}^{K'}$. \mathcal{D}^+ further covers the distribution of actions, providing a foun-
 307 dation for performance scaling.
 308

309 Based on the challenging samples in this enriched dataset, we train the ICM on Round Two (ICM-
 310 r2), using the same cross-entropy loss as defined in Equation 3. This new dataset, which is specif-
 311 ically curated to expose the critic’s most significant blind spots, allows ICM-r2 to acquire a more
 312 nuanced and accurate discriminative ability. Consequently, as illustrated in Figure 3, ICM-r2 pro-
 313 vides more precise guidance for the agent’s action selection, thereby fundamentally strengthening
 314 the critic’s overall judgment and significantly improving the agent’s performance on the most diffi-
 315 cult tasks. Together with ICM, ICM-r2 demonstrates the power of a data flywheel-driven approach
 316 to stimulate the performance of GUI agents during testing.
 317

318 4 EXPERIMENT

319 4.1 IMPLEMENTATION DETAILS

320 **Experimental Setup.** We use UI-TARS 1.0 (Qin et al., 2025) and UI-TARS 1.5 (Qin
 321 et al., 2025) for inference on the AndroidControl (Li et al., 2024) and GUI-Odyssey (Lu
 322 et al., 2024) training sets, and compare the real actions with GT to build \mathcal{D} and \mathcal{D}^+ .
 323

Table 3: **GUI grounding accuracy on ScreenSpotV2.** * indicates reproduced open-source agent performance. \uparrow and \downarrow respectively represent the performance changes relative to the base agents.

Model	Method	Size	Mobile		Desktop		Web		Avg.
			Text	Icon	Text	Icon	Text	Icon	
GPT-4o	ZS	–	30.5	23.2	20.6	19.4	11.1	7.8	18.8
OS-Atlas-Base	ZS	7B	93.0	72.9	91.8	62.9	90.9	74.3	82.5
SeeClick	SFT	9.6B	78.0	52.0	72.2	30.0	55.7	32.5	53.4
Aguvis	SFT	7B	95.6	77.7	93.8	67.1	88.3	75.2	84.4
Qwen 2.5 VL	+ ICM	7B	84.8	59.7	72.1	52.1	69.2	46.3	65.0
			87.9 \uparrow 3.1	70.1 \uparrow 10.4	79.4 \uparrow 7.3	57.1 \uparrow 5.0	74.7 \uparrow 5.5	49.2 \uparrow 2.9	70.4 \uparrow 5.4
			89.7 \uparrow 4.9	68.2 \uparrow 8.5	78.9 \uparrow 6.8	54.3 \uparrow 2.2	76.9 \uparrow 7.7	51.2 \uparrow 4.9	71.1 \uparrow 6.1
UI-TARS 1.0*	+ ICM	7B	93.1	82.4	94.8	76.4	91.8	84.2	88.1
			94.5 \uparrow 1.3	83.1 \uparrow 0.7	93.2 \downarrow 1.6	77.9 \uparrow 1.5	93.5 \uparrow 2.0	84.7 \uparrow 0.5	88.7 \uparrow 0.6
			94.2 \uparrow 1.1	83.7 \uparrow 1.3	95.7 \uparrow 0.9	78.7 \uparrow 2.3	92.1 \uparrow 0.3	84.7 \uparrow 0.5	89.0 \uparrow 0.9
UI-TARS 1.5*	+ ICM	7B	96.2	84.3	94.3	84.2	94.4	86.6	90.8
			96.5 \uparrow 0.3	85.3 \uparrow 1.0	95.4 \uparrow 1.1	84.3 \uparrow 0.1	94.2 \downarrow 0.2	85.2 \downarrow 1.4	90.2 \downarrow 0.6
			97.3 \uparrow 1.1	84.2 \downarrow 0.1	92.4 \downarrow 1.9	84.4 \uparrow 0.2	95.5 \uparrow 1.1	87.7 \uparrow 1.1	91.0 \uparrow 0.2

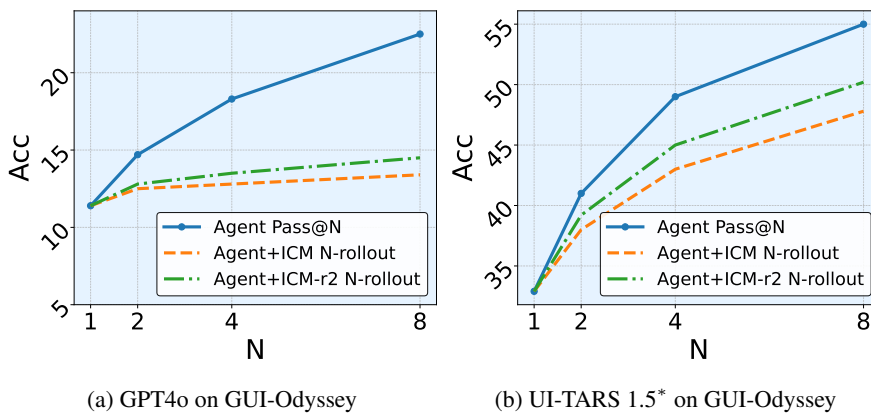
On the corresponding data, we develop the ICM and ICM-r2 based on Qwen2.5 VL 7B (Bai et al., 2025) and adopt the ms-swift (Zhao et al., 2024) framework for training. All action judgments followed the high-level approach, providing only global instructions to the ICM and ICM-r2, not single-step instructions. The distribution of the data flywheel is shown in Table 2. The critic model guides the agents in the N-rollout process with $N = 8$. To allow the base agent to sample a reasonable range of potential actions, its temperature coefficient, top_k, and top_p are set to 1.0, 30, and 0.8, respectively. All experiments are conducted on 8 NVIDIA H100-80G GPUs.

Evaluation. To evaluate the performance of the agent after being guided by the critic model, we evaluate the agent’s task understanding, grounding, and planning capabilities on the AndroidControl and GUI-Odyssey test sets. Furthermore, according to the input, the settings on AndroidControl can be divided into low-level tasks and high-level tasks. High-level tasks only input the global instruction to the agent, while low-level tasks will additionally input the single-step action plan. It should be noted that even for low-level agents, our critic model is guided only by high-level information to ensure the consistency of operation. GUI-Odyssey only adopts the high-level experimental setups. As for the agent’s grounding ability, we measure and compare the performance on ScreenSpotV2 (Cheng et al., 2024).

Comparison. To verify the effectiveness of the proposed evaluation model in guiding existing agent models during testing, we selected a wide range of models. Among the closed-source models, we selected GPT4o (Hurst et al., 2024) and Doubao (UITARS 1.5) (ByteDance, 2025), and implemented action acquisition through API calls. For open source models, we reproduced Qwen 2.5 VL (Bai et al., 2025), UI-TARS 1.0 (Qin et al., 2025), and UI-TARS 1.5 (Qin et al., 2025), where Qwen 2.5 VL is a general multimodal understanding model and UI-TARS is a model fine-tuned for GUI agent tasks. We used the official prompt template to reproduce basic performance and test the superposition evaluation model. The original UI-TARS requires historical actions and up to 5 images of historical steps as input. To simplify the operation, we only let the model refer to the text description of the historical steps and discard the excessive historical image input. For detailed prompt and inference scripts, please refer to the appendix.

Table 2: **Data distribution of the flywheel.** \mathcal{D} and \mathcal{D}^+ respectively represent the data of the first and the second round of GAIA.

Category	Source	Positive	Negative
\mathcal{D}	AndroidControl	68.2k	69.9k
	GUI-Odyssey	65.4k	66.8k
\mathcal{D}^+	AndroidControl	(68.2+15.1)k	(69.9+14.0)k
	GUI-Odyssey	(65.4+26.1)k	(66.8+26.3)k



390 (a) GPT4o on GUI-Odyssey (b) UI-TARS 1.5* on GUI-Odyssey

391

392 Figure 4: Performance improvements of Pass@N and N-rollout.

393

394

395 As a performance comparison, we selected Zero Shot (ZS) model OS-Atlas-Base (Wu et al., 2025c),
 396 SFT-tuned SeeClick (Cheng et al., 2024), Aria-UI (Yang et al., 2024), and Aguvis (Xu et al., 2024),
 397 and RFT-tuned UI-R1 (Lu et al., 2025) and GUI-R1 (Xia & Luo, 2025).

398 **Evaluation Metrics.** For planning tasks, in line with OS-Atlas (Wu et al., 2025c), we report action
 399 type prediction accuracy (Type), click point prediction accuracy (GR), and step success rate (SR).
 400 Specifically: **Type** measures the exact-match accuracy between predicted and ground-truth action
 401 types (e.g., “click” vs. “swipe”). **GR** evaluates grounding performance via click point prediction
 402 accuracy in specific action types (e.g., “click” and “long press”). **SR** is the step-wise success rate:
 403 a step is counted as successful only if both the predicted action and its associated arguments (e.g.,
 404 click coordinates or input text) match the ground truth. For grounding tasks, we use click point
 405 prediction accuracy as our evaluation metric.

4.2 EXPERIMENTAL RESULTS

406 As shown in Table 1, the proposed ICM and ICM-r2 achieve extensive performance improvements
 407 for both zero-shot and fine-tuned GUI agents. On the AndroidControl-High test, ICM can improve
 408 agents’ SR performance by up to 9.3%, while ICM-r2 can further improve it by an average of 1.32%.
 409 The same trend is also observed on GUI-Odyssey, demonstrating that existing models have the
 410 potential to correctly infer actions. ICM can leverage this potential to effectively improve existing
 411 agents during testing, and data flywheels can further amplify these improvements. For agents with
 412 lower basic performance, ICM can significantly improve their performance to an advanced level,
 413 which also demonstrates the potential of the model itself and the stimulation ability of the critic
 414 model. In terms of generalization, GPT4o, Doubao, and Qwen 2.5 VL were not included in the
 415 construction of the GAIA \mathcal{D} and \mathcal{D}^+ , but ICM and ICM-r2 still achieved significant performance
 416 improvements, demonstrating the inherent consistency of real action space data. The real action
 417 sampling in the proposed data flywheel effectively covers this space, providing effective support for
 418 critic training.

419 Both our ICM and ICM-r2 use a high-level approach to judge correctness and guide action, meaning
 420 the critic model is not aware of the current action plan. This setting is more consistent with practical
 421 applications, where only global instructions are given, and the agent must independently reason
 422 about each step’s plan and action. For AndroidControl-Low, the agent is aware of the current action
 423 plan, resulting in higher baseline performance. Despite this, our ICM still achieves a certain degree
 424 of performance improvement, demonstrating the effectiveness of our proposed approach.

425 Table 3 shows the improvement of ICM and ICM-r2 on the grounding ability of agents on
 426 ScreenSpotv2. The ScreenSpotv2 data is not included in the proposed GAIA, and as a single-
 427 step operation, its environmental information is not completely consistent with the aforementioned
 428 datasets. Even so, our evaluation model still improves the performance of agents, which is sufficient
 429 to prove the validity of the data flywheel definition.

430 Please refer to the appendix for more visualization results.

432
433
434
435
436
437
438
439
440
441
442
443
444
445
446
447
448
449
450
451
452
453
454
455
456
457
458
459
460
461
462
463
464
465
466
467
468
469
470
471
472
473
474
475
476
477
478
479
480
481
482
483
484
485

Table 4: **Critic comparison.** The performance is calculated as (Qwen2.5 VL 7B w/ critic) - (Qwen2.5 VL 7B w/o critic).

Model	N	AndroidControl-High		
		Δ Type	Δ GR	Δ SR
UI-Genie-RM	10	–	–	0.3
ICM	8	1.0	5.0	2.8
ICM-r2	8	1.4	5.0	3.2

Table 5: **Impact of differences in critic model attributes on accuracy and guidance.**

Model	Critic Acc	GUI-Odyssey		
		Type	GR	SR
UI-TARS 1.5*	–	71.1	44.6	32.9
	+ RCM	70.82%	75.6	49.2
	+ ICM	83.19%	78.2	52.9
	+ ICM-r2	83.56%	80.2	53.5

4.3 ABLATION STUDY

While utilizing ICM and ICM-r2, we used N -rollout to improve the test-time performance of existing GUI agents, where N is set to 8 by default. To measure the impact of N on final performance, we selected GPT4o and UI-TARS 1.5* as representative closed-source and open-source models, respectively, and compared their SR at different N values on GUI-Odyssey. We also measured the models' Pass@N during the rollout process to reflect the model's performance ceiling. As shown in Figure 4, the increase in Pass@N accuracy reveals the potential of the agents themselves, while the evaluation model approaches this upper limit through N -rollout. The improvement in ICM-r2 and the gap between the upper limit provide potential performance gains for further cycles of GAIA.

4.4 QUALITATIVE EXPERIMENT

Critic Model Comparison. To evaluate the effectiveness of the proposed discriminant model, we compared the accuracy of the Qwen 2.5 VL using a best-of- N approach to guide inference on AndroidControl-High with UI-Genie-RM (Xiao et al., 2025). As shown in Table 4, due to the use of real action data, the proposed ICM significantly improves the accuracy of the base model, and ICM-r2 can further expand the advantage.

Intuitive and Reasoning Critic. To verify that the intuitive judgment proposed in this article is superior, this section implements a critic model based on reinforcement learning design. Specifically, the input of the Reasoning Critic Model (RCM) is consistent with ICM, and the output includes `<thinking>...</thinking>` and `<critic>...</critic>`, which are supervised by format reward and critic reward. **The thought process emerges spontaneously from the model, and the critic reward represents the judgment on the correctness of the current action.** The training of RCM is achieved through Group Relative Policy Optimization (GRPO). Considering the property of reinforcement learning, which is that it can stimulate model capabilities with less data, we randomly sampled 30k data from \mathcal{D}^+ to train RCM. **This setting aligns with existing work on training critic models based on RL Wanyan et al. (2025), ensuring a fair comparison.** This data includes samples from two rounds of GAIA and has the same distribution as the training data for ICM-r2. To intuitively compare the discriminative performance of different critic models, we collected the GAIA test set in a high-level manner on the AndroidControl and GUI-Odyssey test sets in the same way as we collected the training data.

Table 5 shows that the proposed ICM achieves an accuracy of 83.19% for correctness assessment, providing a foundation for action guidance. ICM-r2, benefiting from improved data quality, further achieves an accuracy of 83.56%. In contrast, RCM's classification accuracy is 70.82%, indicating that the thinking component fails to significantly contribute to the final assessment. In terms of action guidance accuracy, while UI-TARS 1.5* under RCM guidance outperforms the original model, it still falls short of ICM. This experimental result demonstrates that intuitive judgment outperforms reasoning for improving agents using a critic model. **Besides, the RCM and GUI-Critic-R1 Wanyan et al. (2025) are required to generate Chain-of-Thought sequences enclosed in `<thinking>` tags before outputting a judgment, often consuming hundreds of tokens. In contrast, the intuitive-based ICM is trained to output a single token ("correct" or "wrong").** This disparity in output length results in an order-of-magnitude reduction in inference latency for ICM. For TTS, which requires evaluating multiple candidates, this efficiency is critical for practical deployment.

486 **5 CONCLUSION**

488 In this work, we addressed the critical challenge of high-stakes, irreversible errors in GUI agents by
 489 proposing a novel framework designed to unleash their latent potential at test time. Our GUI Action
 490 Critic’s Data Flywheel System (GAIA) comprises a data flywheel that iteratively curates a dataset of
 491 realistic action samples and the Intuitive Critic Model (ICM) that evaluates action correctness. This
 492 framework establishes a self-evolutionary cycle: the flywheel continuously enriches its data, which
 493 in turn trains an increasingly powerful critic (ICM-r2). By leveraging a Best-of-N strategy, our ICM
 494 enables agents to select more reliable actions without the need for resource-intensive retraining.
 495 Experimental results on both closed-source and open-source agents demonstrate that GAIA provides
 496 significant performance gains in task planning and grounding capabilities, presenting a promising,
 497 scalable solution for building more robust and intelligent GUI agents.

498 In future work, we will consider unifying high-level and low-level guidance methods and collecting
 499 richer data in online testing, thereby continuously iterating the data flywheel and promoting the
 500 exploration of agent capabilities.

502 **6 ETHICS STATEMENT**

504 The research content of this paper is based on the LVLM GUI Agent. The research process of this
 505 paper does not violate ICLR ethics. There are no discrimination, bias, or fairness issues that need to
 506 be addressed. Our models are not expected to generate potentially harmful content.

508 **7 REPRODUCIBILITY STATEMENT**

510 This article studies a GUI Agent based on LVLM, focusing on proposing a critic model for existing
 511 agent actions. The base model and dataset used in this article are all from open-source and well-
 512 referenced, so this aspect does not affect the reproducibility. To further ensure reproducibility, we
 513 describe the parameters in detail in the main text Section 4.1 and the appendix, and provide prompts
 514 for all models involved in the appendix. We will release the source code and model checkpoints to
 515 support reproducibility.

517 **REFERENCES**

519 Shuai Bai, Keqin Chen, Xuejing Liu, Jialin Wang, Wenbin Ge, Sibo Song, Kai Dang, Peng Wang,
 520 Shijie Wang, Jun Tang, et al. Qwen2.5-VL technical report. *arXiv preprint arXiv:2502.13923*,
 521 2025.

523 Merim Bilalić, Peter McLeod, and Fernand Gobet. Why good thoughts block better ones: The
 524 mechanism of the pernicious *einstellung* (set) effect. *Cognition*, 108(3):652–661, 2008.

525 ByteDance. Doubao. <https://www.volcengine.com/product/doubao>, 2025. Accessed: 2025-8-1.

527 Weize Chen, Jiarui Yuan, Chen Qian, Cheng Yang, Zhiyuan Liu, and Maosong Sun. Optima:
 528 Optimizing effectiveness and efficiency for LLM-based multi-agent system. *arXiv preprint*
 529 *arXiv:2410.08115*, 2024a.

531 Zhe Chen, Weiyun Wang, Yue Cao, Yangzhou Liu, Zhangwei Gao, Erfei Cui, Jinguo Zhu, Shen-
 532 glong Ye, Hao Tian, Zhaoyang Liu, et al. Expanding performance boundaries of open-source
 533 multimodal models with model, data, and test-time scaling. *arXiv preprint arXiv:2412.05271*,
 534 2024b.

535 Kanzhi Cheng, Qiushi Sun, Yougang Chu, Fangzhi Xu, Yantao Li, Jianbing Zhang, and Zhiy-
 536 ong Wu. SeeClick: Harnessing gui grounding for advanced visual GUI agents. *arXiv preprint*
 537 *arXiv:2401.10935*, 2024.

538 Filippos Christianos, Georgios Papoudakis, Thomas Coste, Jianye Hao, Jun Wang, and Kun Shao.
 539 Lightweight neural app control. *arXiv preprint arXiv:2410.17883*, 2024.

540 Tri Dao, Dan Fu, Stefano Ermon, Atri Rudra, and Christopher Ré. FlashAttention: Fast and memory-
 541 efficient exact attention with IO-awareness. *Advances in neural information processing systems*,
 542 35:16344–16359, 2022.

543

544 Julien Doyon and Habib Benali. Reorganization and plasticity in the adult brain during learning of
 545 motor skills. *Current opinion in neurobiology*, 15(2):161–167, 2005.

546

547 Boyu Gou, Ruohan Wang, Boyuan Zheng, Yanan Xie, Cheng Chang, Yiheng Shu, Huan Sun, and
 548 Yu Su. Navigating the digital world as humans do: Universal visual grounding for gui agents.
 549 *arXiv preprint arXiv:2410.05243*, 2024.

550

551 Daya Guo, Dejian Yang, Haowei Zhang, Junxiao Song, Ruoyu Zhang, Runxin Xu, Qihao Zhu,
 552 Shirong Ma, Peiyi Wang, Xiao Bi, et al. DeepSeek-R1: Incentivizing reasoning capability in
 553 LLMs via reinforcement learning. *arXiv preprint arXiv:2501.12948*, 2025.

554

555 Wenyi Hong, Weihan Wang, Qingsong Lv, Jiazheng Xu, Wenmeng Yu, Junhui Ji, Yan Wang, Zihan
 556 Wang, Yuxiao Dong, Ming Ding, et al. CogAgent: A visual language model for GUI agents.
 557 In *Proceedings of the IEEE/CVF Conference on Computer Vision and Pattern Recognition*, pp.
 558 14281–14290, 2024.

559

560 Edward J Hu, Yelong Shen, Phillip Wallis, Zeyuan Allen-Zhu, Yuanzhi Li, Shean Wang, Lu Wang,
 561 Weizhu Chen, et al. LoRA: Low-rank adaptation of large language models. *ICLR*, 1(2):3, 2022.

562

563 Xueyu Hu, Tao Xiong, Biao Yi, Zishu Wei, Ruixuan Xiao, Yurun Chen, Jiasheng Ye, Meiling Tao,
 564 Xiangxin Zhou, Ziyu Zhao, et al. OS Agents: A survey on MLLM-based agents for general
 565 computing devices use, 2024.

566

567 Aaron Hurst, Adam Lerer, Adam P Goucher, Adam Perelman, Aditya Ramesh, Aidan Clark, AJ Os-
 568 trow, Akila Welihinda, Alan Hayes, Alec Radford, et al. Gpt-4o system card. *arXiv preprint
 569 arXiv:2410.21276*, 2024.

570

571 Aaron Jaech, Adam Kalai, Adam Lerer, Adam Richardson, Ahmed El-Kishky, Aiden Low, Alec
 572 Helyar, Aleksander Madry, Alex Beutel, Alex Carney, et al. OpenAI o1 system card. *arXiv
 573 preprint arXiv:2412.16720*, 2024.

574

575 Ziwei Ji, Tiezheng Yu, Yan Xu, Nayeon Lee, Etsuko Ishii, and Pascale Fung. Towards mitigating
 576 LLM hallucination via self reflection. In *Findings of the Association for Computational Linguis-
 577 tics: EMNLP 2023*, pp. 1827–1843, 2023.

578

579 Aditya Kalyanpur, Kailash Karthik Saravanakumar, Victor Barres, Jennifer Chu-Carroll, David
 580 Melville, and David Ferrucci. LLM-ARC: Enhancing LLMs with an automated reasoning critic.
 581 *arXiv preprint arXiv:2406.17663*, 2024.

582

583 Wei Li, William Bishop, Alice Li, Chris Rawles, Folawiyo Campbell-Ajala, Divya Tyamagundlu,
 584 and Oriana Riva. On the effects of data scale on computer control agents. *arXiv e-prints*, pp.
 585 arXiv–2406, 2024.

586

587 Taosheng Liu and Timothy J Pleskac. Neural correlates of evidence accumulation in a perceptual
 588 decision task. *Journal of neurophysiology*, 106(5):2383–2398, 2011.

589

590 Xiao Liu, Bo Qin, Dongzhu Liang, Guang Dong, Hanyu Lai, Hanchen Zhang, Hanlin Zhao, Iat Long
 591 Iong, Jiadai Sun, Jiaqi Wang, et al. Autoglm: Autonomous foundation agents for guis. *arXiv
 592 preprint arXiv:2411.00820*, 2024.

593

594 Yuhang Liu, Pengxiang Li, Zishu Wei, Congkai Xie, Xueyu Hu, Xinchen Xu, Shengyu Zhang,
 595 Xiaotian Han, Hongxia Yang, and Fei Wu. Infiguiagent: A multimodal generalist gui agent with
 596 native reasoning and reflection. *arXiv preprint arXiv:2501.04575*, 2025a.

597

598 Yuhang Liu, Pengxiang Li, Congkai Xie, Xavier Hu, Xiaotian Han, Shengyu Zhang, Hongxia Yang,
 599 and Fei Wu. InfiGUI-R1: Advancing multimodal GUI agents from reactive actors to deliberative
 600 reasoners. *arXiv preprint arXiv:2504.14239*, 2025b.

601

602 Ziyu Liu, Zeyi Sun, Yuhang Zang, Xiaoyi Dong, Yuhang Cao, Haodong Duan, Dahua Lin, and Jiaqi
 603 Wang. Visual-RFT: Visual reinforcement fine-tuning. *arXiv preprint arXiv:2503.01785*, 2025c.

594 Quanfeng Lu, Wenqi Shao, Zitao Liu, Fanqing Meng, Boxuan Li, Botong Chen, Siyuan Huang,
 595 Kaipeng Zhang, Yu Qiao, and Ping Luo. Gui Odyssey: A comprehensive dataset for cross-app
 596 GUI navigation on mobile devices. *arXiv preprint arXiv:2406.08451*, 2024.

597

598 Zhengxi Lu, Yuxiang Chai, Yaxuan Guo, Xi Yin, Liang Liu, Hao Wang, Guanjing Xiong, and
 599 Hongsheng Li. UI-R1: Enhancing action prediction of GUI agents by reinforcement learning.
 600 *arXiv preprint arXiv:2503.21620*, 2025.

601 Ariana Martino, Michael Iannelli, and Coleen Truong. Knowledge injection to counter large
 602 language model (LLM) hallucination. In *European Semantic Web Conference*, pp. 182–185.
 603 Springer, 2023.

604

605 Nat McAleese, Rai Michael Pokorny, Juan Felipe Ceron Uribe, Evgenia Nitishinskaya, Maja Tre-
 606 bacz, and Jan Leike. LLM critics help catch LLM bugs. *arXiv preprint arXiv:2407.00215*, 2024.

607

608 Dang Nguyen, Jian Chen, Yu Wang, Gang Wu, Namyong Park, Zhengmian Hu, Hanjia Lyu, Junda
 609 Wu, Ryan Aponte, Yu Xia, et al. GUI agents: A survey. *arXiv preprint arXiv:2412.13501*, 2024.

610

611 Songqin Nong, Jiali Zhu, Rui Wu, Jiongchao Jin, Shuo Shan, Xiutian Huang, and Wenhao Xu.
 612 Mobileflow: A multimodal LLM for mobile GUI agent. *arXiv preprint arXiv:2407.04346*, 2024.

613

614 Russell A Poldrack, Fred W Sabb, Karin Foerde, Sabrina M Tom, Robert F Asarnow, Susan Y
 615 Bookheimer, and Barbara J Knowlton. The neural correlates of motor skill automaticity. *Journal
 616 of Neuroscience*, 25(22):5356–5364, 2005.

617

618 Mihir Prabhudesai, Tsung-Wei Ke, Alex Li, Deepak Pathak, and Katerina Fragkiadaki. Diffusion-
 619 TTA: Test-time adaptation of discriminative models via generative feedback. *Advances in Neural
 620 Information Processing Systems*, 36:17567–17583, 2023.

621

622 Yujia Qin, Yining Ye, Junjie Fang, Haoming Wang, Shihao Liang, Shizuo Tian, Junda Zhang, Jiahao
 623 Li, Yunxin Li, Shijue Huang, et al. UI-TARS: Pioneering automated GUI interaction with native
 624 agents. *arXiv preprint arXiv:2501.12326*, 2025.

625

626 Haozhan Shen, Peng Liu, Jingcheng Li, Chunxin Fang, Yibo Ma, Jiajia Liao, Qiaoli Shen, Zilun
 627 Zhang, Kangjia Zhao, Qianqian Zhang, et al. VLM-R1: A stable and generalizable R1-style large
 628 vision-language model. *arXiv preprint arXiv:2504.07615*, 2025.

629

630 Huawei Shen, Chang Liu, Gengluo Li, Xinlong Wang, Yu Zhou, Can Ma, and Xiangyang Ji. Falcon-
 631 UI: Understanding GUI before following user instructions. *arXiv preprint arXiv:2412.09362*,
 632 2024.

633

634 Charlie Snell, Jaehoon Lee, Kelvin Xu, and Aviral Kumar. Scaling llm test-time compute optimally
 635 can be more effective than scaling model parameters. *arXiv preprint arXiv:2408.03314*, 2024.

636

637 Charlie Victor Snell, Jaehoon Lee, Kelvin Xu, and Aviral Kumar. Scaling LLM test-time com-
 638 plete optimally can be more effective than scaling parameters for reasoning. In *The Thirteenth
 639 International Conference on Learning Representations*, 2025.

640

641 Yunpeng Song, Yiheng Bian, Yongtao Tang, Guiyu Ma, and Zhongmin Cai. Visiontasker: Mobile
 642 task automation using vision based ui understanding and llm task planning. In *Proceedings of the
 643 37th Annual ACM Symposium on User Interface Software and Technology*, pp. 1–17, 2024.

644

645 Fei Tang, Yongliang Shen, Hang Zhang, Siqi Chen, Guiyang Hou, Wenqi Zhang, Wenqiao Zhang,
 646 Kaitao Song, Weiming Lu, and Yueteng Zhuang. Think twice, click once: Enhancing GUI ground-
 647 ing via fast and slow systems. *arXiv preprint arXiv:2503.06470*, 2025.

648

649 Xiaoyu Tian, Sitong Zhao, Haotian Wang, Shuaiting Chen, Yunjie Ji, Yiping Peng, Han Zhao, and
 650 Xiangang Li. Think twice: Enhancing LLM reasoning by scaling multi-round test-time thinking.
 651 *arXiv preprint arXiv:2503.19855*, 2025.

652

653 Xiaohong Wan, Hironori Nakatani, Kenichi Ueno, Takeshi Asamizuya, Kang Cheng, and Keiji
 654 Tanaka. The neural basis of intuitive best next-move generation in board game experts. *Science*,
 655 331(6015):341–346, 2011.

648 Peng Wang, Shuai Bai, Sinan Tan, Shijie Wang, Zhihao Fan, Jinze Bai, Keqin Chen, Xuejing Liu,
 649 Jialin Wang, Wenbin Ge, et al. Qwen2-VL: Enhancing vision-language model’s perception of the
 650 world at any resolution. *arXiv preprint arXiv:2409.12191*, 2024a.

651

652 Shuai Wang, Weiwen Liu, Jingxuan Chen, Yuqi Zhou, Weinan Gan, Xingshan Zeng, Yuhan Che,
 653 Shuai Yu, Xinlong Hao, Kun Shao, et al. GUI agents with foundation models: A comprehensive
 654 survey. *arXiv preprint arXiv:2411.04890*, 2024b.

655 Yutong Wang, Pengliang Ji, Chaoqun Yang, Kaixin Li, Ming Hu, Jiaoyang Li, and Guillaume Sar-
 656 toretti. MCTS-judge: Test-time scaling in LLM-as-a-judge for code correctness evaluation. *arXiv*
 657 *preprint arXiv:2502.12468*, 2025.

658

659 Yuyang Wanyan, Xi Zhang, Haiyang Xu, Haowei Liu, Junyang Wang, Jiabo Ye, Yutong Kou, Ming
 660 Yan, Fei Huang, Xiaoshan Yang, et al. Look before you leap: A GUI-Critic-R1 model for pre-
 661 operative error diagnosis in GUI automation. *arXiv preprint arXiv:2506.04614*, 2025.

662 Muning Wen, Ziyu Wan, Jun Wang, Weinan Zhang, and Ying Wen. Reinforcing LLM agents via
 663 policy optimization with action decomposition. *Advances in Neural Information Processing Sys-
 664 tems*, 37:103774–103805, 2024.

665

666 Hang Wu, Hongkai Chen, Yujun Cai, Chang Liu, Qingwen Ye, Ming-Hsuan Yang, and Yiwei Wang.
 667 DiMo-GUI: Advancing test-time scaling in gui grounding via modality-aware visual reasoning.
 668 *arXiv preprint arXiv:2507.00008*, 2025a.

669

670 Qianhui Wu, Kanzhi Cheng, Rui Yang, Chaoyun Zhang, Jianwei Yang, Huiqiang Jiang, Jian Mu,
 671 Baolin Peng, Bo Qiao, Reuben Tan, et al. GUI-Actor: Coordinate-free visual grounding for GUI
 672 agents. *arXiv preprint arXiv:2506.03143*, 2025b.

673

674 Zhiyong Wu, Zhenyu Wu, Fangzhi Xu, Yian Wang, Qiushi Sun, Chengyou Jia, Kanzhi Cheng,
 675 Zichen Ding, Liheng Chen, Paul Pu Liang, et al. OS-ATLAS: A foundation action model for
 676 generalist GUI agents. In *International Conference on Learning Representations*, 2025c.

677

678 Xiaobo Xia and Run Luo. GUI-R1: A generalist R1-style vision-language action model for GUI
 679 agents. *arXiv preprint arXiv:2504.10458*, 2025.

680

681 Han Xiao, Guozhi Wang, Yuxiang Chai, Zimu Lu, Weifeng Lin, Hao He, Lue Fan, Liuyang Bian,
 682 Rui Hu, Liang Liu, et al. UI-Genie: A self-improving approach for iteratively boosting MLLM-
 683 based mobile GUI agents. *arXiv preprint arXiv:2505.21496*, 2025.

684

685 Tianyi Xiong, Xiayao Wang, Dong Guo, Qinghao Ye, Haoqi Fan, Quanquan Gu, Heng Huang, and
 686 Chunyuan Li. LLaVA-Critic: Learning to evaluate multimodal models. In *Proceedings of the*
 687 *Computer Vision and Pattern Recognition Conference*, pp. 13618–13628, 2025.

688

689 Yiheng Xu, Zekun Wang, Junli Wang, Dunjie Lu, Tianbao Xie, Amrita Saha, Doyen Sahoo, Tao Yu,
 690 and Caiming Xiong. Aguviz: Unified pure vision agents for autonomous GUI interaction. *arXiv*
 691 *preprint arXiv:2412.04454*, 2024.

692

693 Jianwei Yang, Hao Zhang, Feng Li, Xueyan Zou, Chunyuan Li, and Jianfeng Gao. Set-of-Mark
 694 prompting unleashes extraordinary visual grounding in GPT-4V, 2023. URL <https://arxiv.org/abs/2310.11441>.

695

696 Yan Yang, Dongxu Li, Yutong Dai, Yuhao Yang, Ziyang Luo, Zirui Zhao, Zhiyuan Hu, Junzhe
 697 Huang, Amrita Saha, Zeyuan Chen, et al. GTA1: GUI test-time scaling agent. *arXiv preprint*
 698 *arXiv:2507.05791*, 2025.

699

700 Yuhao Yang, Yue Wang, Dongxu Li, Ziyang Luo, Bei Chen, Chao Huang, and Junnan Li. Aria-UI:
 701 Visual grounding for GUI instructions. *arXiv preprint arXiv:2412.16256*, 2024.

702

703 Di Zhang, Jingdi Lei, Junxian Li, Xunzhi Wang, Yujie Liu, Zonglin Yang, Jiatong Li, Weida Wang,
 704 Suorong Yang, Jianbo Wu, et al. Critic-V: VLM critics help catch VLM errors in multimodal
 705 reasoning. In *Proceedings of the Computer Vision and Pattern Recognition Conference*, pp. 9050–
 706 9061, 2025a.

702 Ziyao Zhang, Chong Wang, Yanlin Wang, Ensheng Shi, Yuchi Ma, Wanjun Zhong, Jiachi Chen,
703 Mingzhi Mao, and Zibin Zheng. LLM hallucinations in practical code generation: Phenomena,
704 mechanism, and mitigation. *Proceedings of the ACM on Software Engineering*, 2(ISSTA):481–
705 503, 2025b.

706 Yuze Zhao, Jintao Huang, Jinghan Hu, Xingjun Wang, Yunlin Mao, Daoze Zhang, Zeyinzi Jiang,
707 Zhikai Wu, Baole Ai, Ang Wang, Wenmeng Zhou, and Yingda Chen. SWIFT:a scalable
708 lightweight infrastructure for fine-tuning, 2024. URL <https://arxiv.org/abs/2408.05517>.

711 Jiani Zheng, Lu Wang, Fangkai Yang, Chaoyun Zhang, Lingrui Mei, Wenjie Yin, Qingwei Lin,
712 Dongmei Zhang, Saravan Rajmohan, and Qi Zhang. VEM: Environment-free exploration for
713 training gui agent with value environment model. *arXiv preprint arXiv:2502.18906*, 2025.

714

715

716

717

718

719

720

721

722

723

724

725

726

727

728

729

730

731

732

733

734

735

736

737

738

739

740

741

742

743

744

745

746

747

748

749

750

751

752

753

754

755

756 A CLARIFICATION OF THE USAGE OF LLMs
757758 This paper only used LLMs to assist and polish the writing. The retrieval, core innovation, method
759 design, and experiments related to the paper were not conducted with the help of LLMs.
760761 B INFERENCE PROMPTS
762764 In this section, we introduce the inference parameters and prompt template of the LVLM used. The
765 proposed GAIA data flywheel and trained ICM are used to guide existing GUI agents at test time.
766 GAIA data is also constructed using the action reasoning of existing agents.
767768 B.1 GUI AGENT PLANNING TASK PROMPTS
769770 **GPT4o** We use the API to test the closed-source model GPT4o (Hurst et al., 2024) as a GUI agent.
771 Prompts refer to UI-TARS 1.0 (Qin et al., 2025) to ensure consistency in the action space. System
772 prompts and user prompts refer to Prompt 1 and Prompt 3. The “You need to: {step_plan}” in User
773 Prompt is only used when testing AndroidControl-Low (Li et al., 2024). In other conditions, the
774 agent will not receive specific step instructions.
775776 **Doubaot** Doubaot, ByteDance’s closed-source model interface, provides a closed-source version of
777 UI-TARS 1.5, which represents the most advanced GUI agent. We test the performance of closed-
778 source UI-TARS 1.5 by calling Doubaot’s API (ByteDance, 2025). The Prompt used for the test is
779 consistent with the open source version UI-TARS 1.5 (Qin et al., 2025), see Prompt 2 and Prompt 3.
780 The “You need to: {step_plan}” in User Prompt is only used when testing AndroidControl-Low. In
781 other conditions, the Agent will not receive specific step instructions.
782783 **UI-TARS 1.0*** For UI-TARS 1.0 (Qin et al., 2025), we use the open source weight UI-TARS-7B-
784 DPO for testing. System prompts and user prompts refer to Prompt 1 and Prompt 3. The “You need to:
785 {step_plan}” in User Prompt is only used when testing AndroidControl-Low. In other conditions,
786 the agent will not receive specific step instructions. It should be noted that UI-TARS can receive up
787 to five historical images as input. To simplify the process, we only use the text of “action_history”
788 to describe the historical steps. For the image, we only input the current screenshot.
789790 **UI-TARS 1.5*** For UI-TARS 1.5 (Qin et al., 2025), we use the open source weight UI-TARS-1.5-7B
791 for testing. System prompts and user prompts refer to Prompt 2 and Prompt 3. The “You need to:
792 {step_plan}” in User Prompt is only used when testing AndroidControl-Low. In other conditions,
793 the agent will not receive specific step instructions. It should be noted that UI-TARS 1.5 can receive
794 up to five historical images as input. To simplify the process, we only use the text of “action_history”
795 to describe the historical steps. For the image, we only input the current screenshot.
796797 **Qwen 2.5 VL** For Qwen 2.5 VL (Bai et al., 2025), we use the open source weight Qwen-2.5-VL-
798 7B-Instruct for testing. We refer to the official use case and use the function calls to test Qwen’s
799 GUI Agent capabilities. The prompt is shown in Prompt 4 and 5.
800801 B.2 GUI AGENT GROUNDING TASK PROMPTS
802803 Grounding capabilities are tested on the ScreenSpotV2 (Cheng et al., 2024) dataset. Because
804 Grounding only provides single-step instructions and screenshots, and operations only involve click
805 locations, the Prompts in Grounding differ from those in planning. The prompts for UI-TARS 1.0*
806 and UI-TARS 1.5* refer to Prompt 6 and Prompt 7 respectively. The Qwen 2.5 VL test also applies
807 function calls and constrains its output format through JSON, where Prompt is shown in Prompt 4
808 and 5. Prompt is the same as planning task, but without “action_history”.
809810 B.3 ICM PROMPTS
811812 The ICM and ICM-r2 trained on GAIA follow the same prompt and make judgments across the
813 full action space. Therefore, the same prompt is used for both Planning and Grounding, as shown
814 in Prompt 8. The information of “global_instruction” and “action_history” is consistent with that
815 obtained by the basic GUI agent. “actor_set” describes the current action. If the action is click or
816

810 long press, it is constructed as “Tap at [x, y]”, where x and y are the absolute coordinates of the
 811 click position in the original image. If the action is swipe, “actor_set” is constructed as “Swipe to
 812 up/down/left/right”. If the action is type or open, “actor_set” is constructed as “Type/Open [text]”,
 813 where [text] is the input text or the name of the App to be opened. The other actions have no param-
 814 eters, so “actor_set” is directly the action name, such as “Wait”, “Home”, “Back”, etc.

815 For the input image, we refer to the Set-of-Mark (SoM) approach (Yang et al., 2023). If the action is
 816 click or long press, a red circle is drawn at the click location. Otherwise, the original image is used
 817 directly as the ICM reference. The model’s attention is implemented using FlashAttention (Dao
 818 et al., 2022). The data type is bfloat16. The epoch is 1, and the batch size is 16.
 819

820 C TRAINING PARAMETERS

821 Using GAIA data, we train ICM and ICM-r2 with the following parameters. We fine-tune Qwen
 822 2.5 VL 7B by inserting LoRA (Hu et al., 2022) into all linear layers, with lora_rank set to 8 and
 823 lora_alpha set to 32. The epoch is 1, and the batch size is 16. The optimizer is AdamW with a
 824 learning rate of 1e-4 and a warmup ratio of 0.05.
 825

826 D BEST-OF-N METHOD

827 ICM and ICM-r2 use the Best-of-N approach to select the correct action with the highest probability
 828 from the N actions in the GUI agent rollout as the actual output, where the probability is expressed
 829 as the probability of the “correct” token. The core code of this process is shown in Code 1.
 830

831 E VISUALIZATION RESULTS

832 We show the actions of the basic GUI agents on the sample, as well as the actions after being guided
 833 by ICM and ICM-r2. The comparison is shown in Figure 5 to 8.
 834

835
 836
 837
 838
 839
 840
 841
 842
 843
 844
 845
 846
 847
 848
 849
 850
 851
 852
 853
 854
 855
 856
 857
 858
 859
 860
 861
 862
 863

```

864
865
866
867
868
869
870
871
872
873
874
875
876
877 GPT4o and UI-TARS 1.0* System GUI Prompt
878 You are a GUI agent. You are given a task and your
879 action history, with screenshots. You need to perform
880 the next action to complete the task.
881
882 ## Output Format
883 Thought: ...
884 Action: ...
885
886 ## Action Space
887
888 click(point='(x1 y1)')
889 long_press(point='(x1 y1)')
890 type(content='')
891 scroll(point='(x1 y1)', direction='down or up or right or left')
892 open_app(app_name='\'')
893 drag(start_point='(x1 y1)', end_point='(x2 y2)')
894 press_home()
895 press_back()
896 finished(content='xxx')
897
898 ## Note
899 - Use English in Thought part.
900 - Summarize your next action (with its target element) in one
901 sentence in Thought part.
902
903 ## User Instruction
904
905 Prompt 1: GPT4o and UI-TARS 1.0* System GUI Prompt
906
907
908
909
910
911
912
913
914
915
916
917

```

918
919
920
921 **Doubao[†] and UI-TARS 1.5* System GUI Prompt**
922
923 You are a GUI agent. You are given a task and your
924 action history, with screenshots. You need to perform
925 the next action to complete the task.
926
927 ## Output Format
928 Thought: ...
929 Action: ...
930
931 ## Action Space
932
933 click(point='<|box_start|>(x1 y1)<|box_end|>')
934 long_press(point='<|box_start|>(x1 y1)<|box_end|>')
935 type(content='')
936 scroll(point='<|box_start|>(x1 y1)<|box_end|>',
937 direction='down or up or right or left')
938 open_app(app_name='\')
939 drag(start_point='<|box_start|>(x1 y1)<|box_end|>',
940 end_point='<|box_start|>(x2 y2)<|box_end|>')
941 press_home()
942 press_back()
943 finished(content='xxx')
944
945 ## Note
946 - Use English in Thought part.
947 - Summarize your next action (with its target element) in one
948 sentence in Thought part.
949
950 ## User Instruction

Prompt 2: Doubao[†] and UI-TARS 1.5* System GUI Prompt

GPT4o, DouBao[†], UI-TARS 1.0* and UI-TARS 1.5* User GUI Prompt

- User Instruction
{global_instruction} (You need to: {step_plan})
- Action History
{action_history}
- Current Screenshot
{image_path}

Prompt 3: GPT4o, Doubao[†], UI-TARS 1.0* and UI-TARS 1.5* User GUI Prompt

```

972
973 Qwen 2.5 VL GUI and Grounding Prompt
974 You are a GUI Agent.
975
976 # Tools
977
978 You may call one or more functions to assist with the user query.
979
980 You are provided with function signatures within <tools></tools>
981 XML tags:
982 <tools>
983 {"type": "function",
984     "function": {
985         "name": "mobile_use", "description": "Use a touchscreen to
986         interact with a mobile device, and take screenshots.
987         * This is an interface to a
988         mobile device with touchscreen. You can perform actions like
989         clicking, typing, swiping, etc.
990         * Some applications may take time to start or
991         process actions, so you may need to wait and take successive
992         screenshots to see the results of your actions.
993         * The screen\'s resolution is 1092x2408.
994         * Make sure to click any buttons, links, icons, etc with the
995
996             cursor tip in the center of the element. Don't click boxes
997             on their edges unless asked.",
998         "parameters": {
999             "properties": {
1000                 "action": {
1001                     "description": "The action to perform. The available
1002                     actions are:
1003                     * 'key': Perform a key event on the mobile device.
1004                     - This supports adb\'s 'keyevent' syntax.
1005                     - Examples: \\\"volume_up\\\", \\\"volume_down\\\", \\\"power\\\",
1006                     \\\"camera\\\", \\\"clear\\\".
1007                     * 'click': Click the point on the screen with
1008                     coordinate (x, y).
1009                     * 'long_press': Press the point on the screen with coordinate
1010                     (x, y) for specified seconds.
1011                     * 'swipe': Swipe from the starting point with coordinate
1012                     (x, y) to the end point with coordinates2 (x2, y2).
1013                     * 'type': Input the specified text into the activated
1014                     input box.
1015                     * 'system_button': Press the system button.
1016                     * 'open': Open an app on the device.
1017                     * 'wait': Wait specified seconds for the change to happen.
1018                     * 'terminate': Terminate the current task and report its
1019
1020             completion status.",
1021             "enum": ["key", "click", "long_press", "swipe", "type",
1022             "system_button", "open", "wait", "terminate"],
1023             "type": "string
1024         },
1025

```

Prompt 4: Qwen 2.5 VL GUI and Grounding Prompt

```

1026
1027
1028
1029
1030 Qwen 2.5 VL GUI and Grounding Prompt (cont.)
1031
1032     "coordinate": {"description": "(x, y): The x (pixels from
1033         the left edge) and y (pixels from the top edge)
1034         coordinates to move the mouse to. Required only by
1035         'action=click', 'action=long_press', and 'action=swipe'.",
1036         "type": "array"},

1037     "coordinate2": {"description": "(x, y): The x (pixels from
1038         the left edge) and y (pixels from the top edge)
1039         coordinates to move the mouse to. Required only by
1040         'action=swipe'."}, "type": "array"},

1041     "text": {"description": "Required only by 'action=key',
1042         'action=type', and 'action=open'."}, "type": "string"},

1043     "time": {"description": "The seconds to wait. Required only
1044         by 'action=long_press' and 'action=wait'."},
1045         "type": "number"},

1046     "button": {"description": "Back means returning to the
1047         previous interface, Home means returning to the desktop,
1048         Menu means opening the application background menu,
1049         and Enter means pressing the enter. Required only
1050         by 'action=system_button'."},

1051     "enum": ["Back", "Home", "Menu", "Enter"], "type": "string"},

1052     "status": {
1053         "description": "The status of the task. Required only
1054
1055             by 'action=terminate'."}, "type": "string", "enum": ["success", "failure"]
1056     }
1057     "required": ["action"], "type": "object"
1058 }
1059 }
1060 
```

1061 </tools>

1062 For each function call, return a json object with function name
1063 and arguments within <tool_call></tool_call> XML tags:
1064 <tool_call>
1065 {"name": <function-name>, "arguments": <args-json-object>}
1066 </tool_call>

1067 The user query:
1068 {global_instruction}
1069 Task progress (You have done the following operation on
1070 the current device):
1071 {action_history}

1072 {image_path}

1073

1074

1075 **Prompt 5: Qwen 2.5 VL GUI and Grounding Prompt (cont.)**

1076

1077

1078

1079

1080
1081
1082
1083

UI-TARS 1.0* GUI Grounding Prompt

1084
1085
1086 You are a GUI agent. You are given a task and your action
1087 history, with screenshots. You need to perform the next
1088 action to complete the task.
1089
1090 ## Output Format
1091
1092 Action: ...
1093
1094
1095 ## Action Space
1096 click(point='<point>x1 y1</point>')
1097
1098 ## User Instruction
1099 {instruction}
1100
1101 {image_path}

Prompt 6: UI-TARS 1.0* GUI Grounding Prompt

1103
1104
1105
1106
1107
1108
1109
1110

UI-TARS 1.5* GUI Grounding Prompt

1111
1112
1113 You are a GUI agent. You are given a task and your action
1114 history, with screenshots. You need to perform the next
1115 action to complete the task.
1116
1117 ## Output Format
1118
1119 Action: ...
1120
1121
1122 ## Action Space
1123 click(point='<|box_start|>(x1,y1)<|box_end|>')
1124
1125 ## User Instruction
1126 {instruction}
1127
1128 {image_path}

Prompt 7: UI-TARS 1.5* GUI Grounding Prompt

1129
1130
1131
1132
1133

```

1134
1135
1136
1137
1138
1139
1140
1141
1142
1143
1144
1145
1146 ICM and ICM-r2 Critic Prompt
1147 You are an expert in evaluating the performance of a phone
1148 operating agent. The agent is designed to help a user to
1149 complete a task or retrieve information from the phone.
1150 Given the user's task instruction, current action and current
1151 screenshot, your goal is to decide whether the agent's current
1152 action is correct or not.
1153 Each action in the sequence is preceded by a corresponding
1154 screenshot that captures the context in which the action occurs.
1155 ## Evaluation Criteria
1156 Whether the agent's current action is correct and corresponding
1157 to the user's task instruction.
1158
1159 ## IMPORTANT
1160 1. An action always follows a corresponding screenshot (even if
1161 only the last few are provided).
1162 2. If the current action is a tap on the screen, the point where
1163 the action is clicked is marked with a red circle on
1164 the screenshot.
1165 3. You should whether answer [correct] or [wrong].
1166 ## Input
1167
1168 The input is given next, including global_task_instruction,
1169 action_history, current_action, and screenshot.
1170 The goal of the task (instruction): {global_instruction}
1171 Action (plan) history: {action_history}
1172 Current action of the agent: {actor_set}
1173 Screenshot: {som_image_path}
1174
1175 Prompt 8: ICM and ICM-r2 Critic Prompt
1176
1177
1178
1179
1180
1181
1182
1183
1184
1185
1186
1187

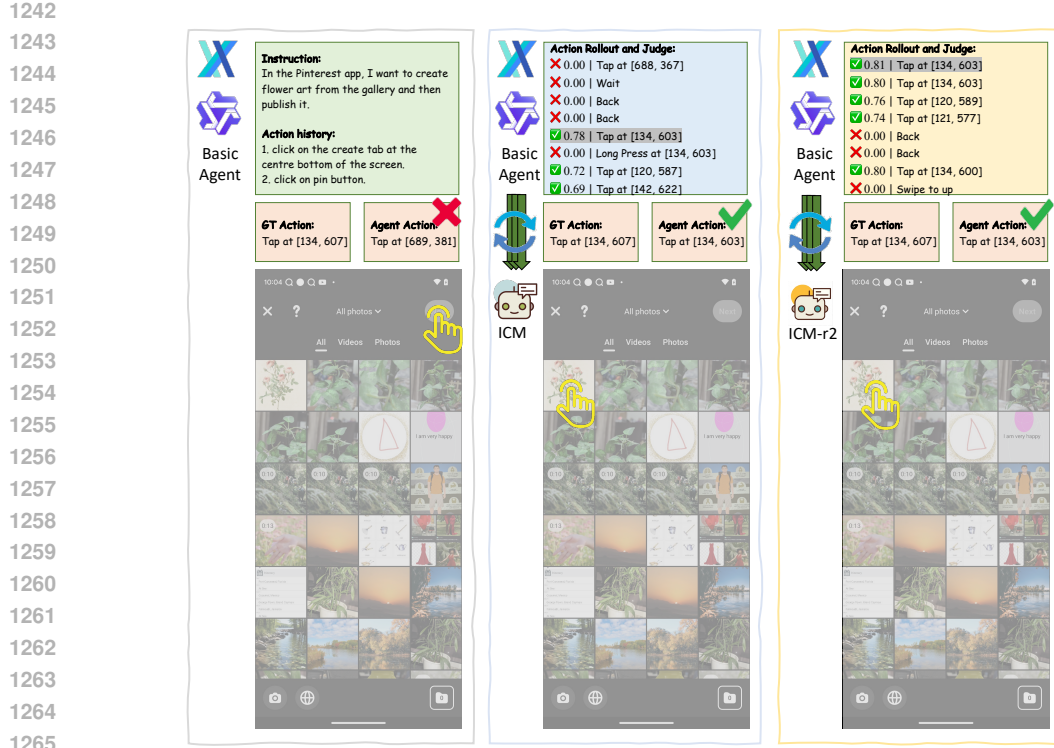
```

```

1188
1189
1190
1191
1192
1193 Best-of-N Example Code
1194
1195     # 1. construct critic input
1196     texts = [
1197         critic_processor.apply_chat_template(msg, tokenize=False,
1198         add_generation_prompt=True) for msg in messages
1199     ]
1200     image_inputs, video_inputs = process_vision_info(messages)
1201     inputs = critic_processor(
1202         text=texts,
1203         images=image_inputs,
1204         videos=video_inputs,
1205         padding=True,
1206         return_tensors="pt",
1207     )
1208     inputs = inputs.to(critic_device)
1209
1210     # 2. generate output
1211     output = critic_model.generate(**inputs,
1212         do_sample=False,
1213         max_new_tokens=2048,
1214         return_dict_in_generate=True,
1215         output_scores=True)
1216     generated_ids = output.sequences
1217
1218     # 3. get token score
1219     scores = output.scores[0]
1220     critic_scores = scores[:, -2]
1221
1222     # 4. get output text: correct|wrong
1223     for in_ids, out_ids in zip(inputs.input_ids, generated_ids):
1224         generated_ids_trimmed = [out_ids[len(in_ids):]]
1225     responses = critic_processor.batch_decode(
1226         generated_ids_trimmed, skip_special_tokens=True,
1227         clean_up_tokenization_spaces=False
1228     )
1229
1230     # 5. find the index of the best action
1231     max_score = -float('inf')
1232     best_idx = -1
1233     for idx in range(len(critic_outputs)):
1234         if responses[idx] == 'correct':
1235             if critic_scores[idx] > max_score:
1236                 max_score = critic_scores[idx]
1237                 best_idx = idx
1238
1239
1240
1241

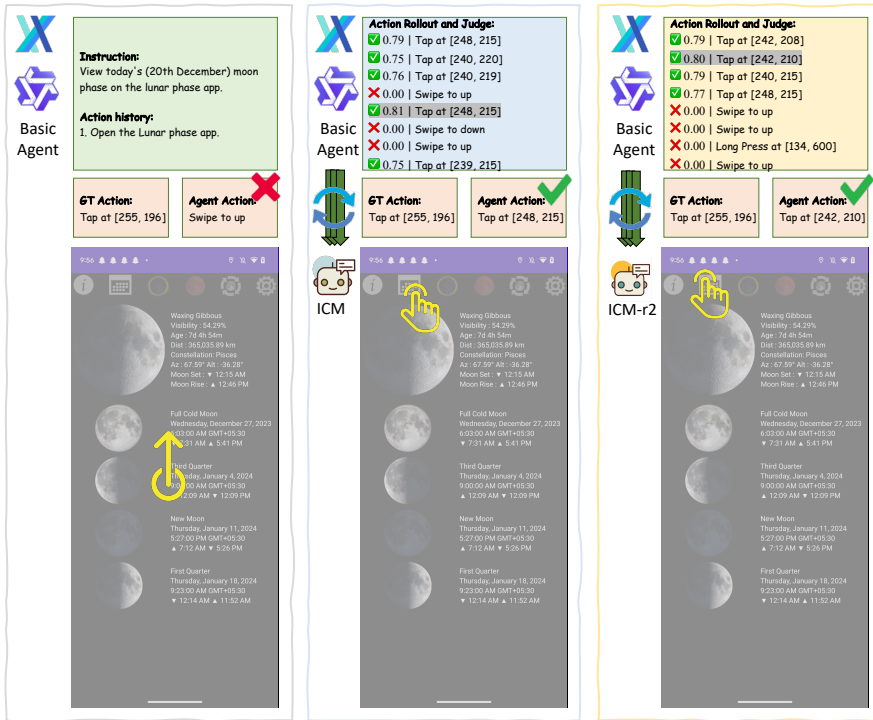
```

Code 1: Best-of-N Example Code



1266
1267
1268
1269
1270
1271
1272
1273
1274
1275
1276
1277
1278
1279
1280
1281
1282
1283
1284
1285
1286
1287
1288
1289
1290
1291
1292
1293

Figure 5: **Visualization result.** The basic agent selects the wrong action. Based on the action rollout, both ICM and ICM-r2 select the correct action from the candidates.



1294
1295

Figure 6: **Visualization result.** The basic agent selects the wrong action. Based on the action rollout, both ICM and ICM-r2 select the correct action from the candidates.

1296

1297

1298

1299

1300

1301

1302

1303

1304

1305

1306

1307

1308

1309

1310

1311

1312

1313

1314

1315

1316

1317

1318

1319

1320

1321

1322

1323

1324

1325

1326

1327

1328

1329

1330

1331

1332

1333

1334

1335

1336

1337

1338

1339

1340

1341

1342

1343

1344

1345

1346

1347

1348

1349

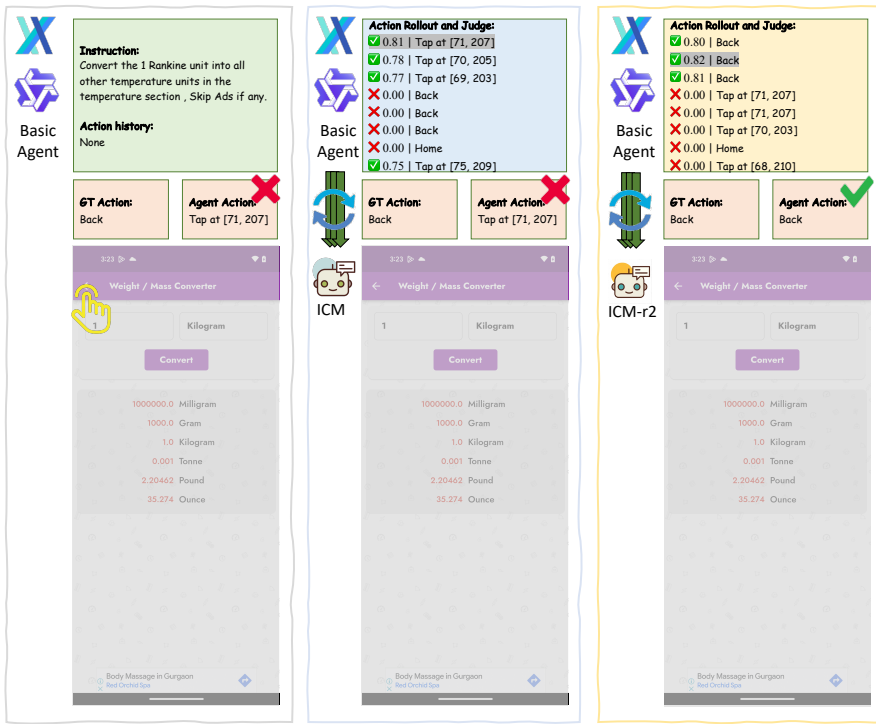


Figure 7: **Visualization result.** The basic agent selects the wrong action. ICM fails to select the correct one from the rollout candidates, while the enhanced ICM-r2 guides the correct selection.

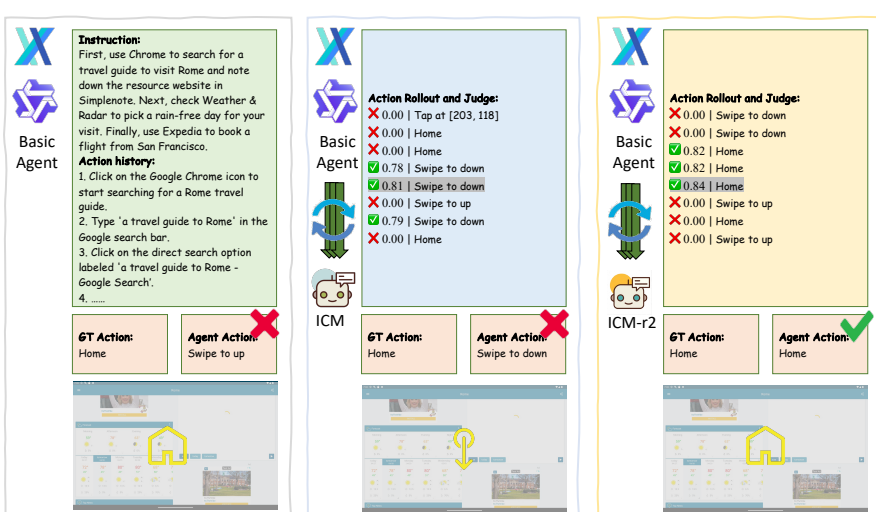


Figure 8: **Visualization result.** The basic agent selects the wrong action. ICM fails to select the correct one from the rollout candidates, while the enhanced ICM-r2 guides the correct selection.